

Photovoltaic electrical properties of aqueous grown ZnO antireflective nanostructure on Cu(In,Ga)Se₂ thin film solar cells

Yi-Chih Wang,^{1,*} Bing-Yi Lin,² Po-Tsun Liu,³
and Han-Ping D. Shieh³

¹Department of Photonics and Institute of Electro-optical Engineering, National Chiao Tung University, Ta-Hsueh Rd., Hsinchu 30010, Taiwan

²College of Photonics and Institute of Lighting and Energy Photonics, National Chiao Tung University, Gaofa 3rd Rd., Tainan 71150, Taiwan

³Department of Photonics and Display Institute, National Chiao Tung University, Ta-Hsueh Rd., Hsinchu 30010, Taiwan

*easonwang.eo98g@g2.nctu.edu.tw

Abstract: A solution-grown subwavelength antireflection coating has been investigated for enhancing the photovoltaic efficiency of thin film solar cells. The 100-nm-height ZnO nanorods coating benefited the photocurrent of Cu(In,Ga)Se₂ solar cells from 31.7 to 34.5 mA/cm² via the decrease of surface light reflectance from 14.5% to 7.0%, contributed by the gradual refractive index profile between air and AZO window layer. The further reduction of surface reflectance to 2.3% in the case of 540-nm-height nanorods, yet, lowered the photocurrent to 29.5 mA/cm², attributed to the decrease in transmittance. The absorption effect of hydrothermal grown ZnO nanorods was explored to optimize the antireflection function in enhancing photovoltaic performances.

©2013 Optical Society of America

OCIS codes: (040.5350) Photovoltaic; (350.6050) Solar energy; (310.1210) Antireflection coating.

References and links

1. Y. K. Liao, S. Y. Kuo, W. T. Lin, F. I. Lai, D. H. Hsieh, M. A. Tsai, S. C. Chen, D. W. Chiou, J. C. Chang, K. H. Wu, S. J. Cheng, and H.-C. Kuo, "Observation of unusual optical transitions in thin-film Cu(In,Ga)Se₂ solar cells," *Opt. Express* **20**(S6), A836–A842 (2012).
2. X. H. Tan, S. L. Ye, and X. Liu, "Increasing surface band gap of Cu(In,Ga)Se₂ thin films by post depositing an In-Ga-Se thin layer," *Opt. Express* **19**(7), 6609–6615 (2011).
3. Y. C. Wang and H. P. Shieh, "Improvement of bandgap homogeneity in Cu(In,Ga)Se₂ thin films using a modified two-step selenization process," *Appl. Phys. Lett.* **103**(15), 153502 (2013).
4. R. Caballero, C. Guillén, M. Gutiérrez, and C. A. Kaufmann, "CuIn_{1-x}Ga_xSe₂-based thin-film solar cells by the selenization of sequentially evaporated metallic layers," *Prog. Photovolt. Res. Appl.* **14**(2), 145–153 (2006).
5. V. Gremenok, E. Zaretskaya, V. Zaleski, K. Bente, W. Schmitz, R. Martin, and H. Moller, "Preparation of Cu(In,Ga)Se₂ thin film solar cells by two-stage selenization processes using N₂ gas," *Sol. Energy Mater. Sol. Cells* **89**(2–3), 129–137 (2005).
6. C. H. Huang, H. L. Cheng, W. E. Chang, and M. S. Wong, "Comprehensive characterization of DC sputtered AZO films for CIGS photovoltaics," *J. Electrochem. Soc.* **158**(5), H510–H515 (2011).
7. M. Y. Hsieh, S. Y. Kuo, H. V. Han, J. F. Yang, Y. K. Liao, F. I. Lai, and H. C. Kuo, "Enhanced broadband and omnidirectional performance of Cu(In,Ga)Se₂ solar cells with ZnO functional nanotree arrays," *Nanoscale* **5**(9), 3841–3846 (2013).
8. B. K. Shin, T. I. Lee, J. Xiong, C. Hwang, G. Noh, J. H. Cho, and J. M. Myoung, "Bottom-up grown ZnO nanorods for an antireflective moth-eye structure on CuInGaSe₂ solar cells," *Sol. Energy Mater. Sol. Cells* **95**(9), 2650–2654 (2011).
9. L. Aé, D. Kieven, J. Chen, R. Klenk, T. Rissom, Y. Tang, and M. C. Lux-Steiner, "ZnO nanorod arrays as an antireflective coating for Cu(In,Ga)Se₂ thin film solar cells," *Prog. Photovolt. Res. Appl.* **18**(3), 209–213 (2010).
10. S. Y. Kuo, M. Y. Hsieh, F. I. Lai, Y. K. Liao, M. H. Kao, and H. C. Kuo, "Modeling and optimization of sub-wavelength grating nanostructures on Cu(In,Ga)Se₂ solar cell," *Jpn. J. Appl. Phys.* **51**, 10NC14 (2012).
11. S. H. Baek, B. Y. Noh, I. K. Park, and J. H. Kim, "Fabrication and characterization of silicon wire solar cells having ZnO nanorod antireflection coating on Al-doped ZnO seed layer," *Nanoscale Res. Lett.* **7**(1), 29 (2012).

12. Y. L. Chen, L. C. Kuo, M. L. Tseng, H. M. Chen, C. K. Chen, H. J. Huang, R. S. Liu, and D. P. Tsai, "ZnO nanorod optical disk photocatalytic reactor for photodegradation of methyl orange," *Opt. Express* **21**(6), 7240–7249 (2013).
13. I. H. Choi, "Raman spectroscopy of $\text{CuIn}_{1-x}\text{Ga}_x\text{Se}_2$ for in-situ monitoring of the composition ratio," *Thin Solid Films* **519**(13), 4390–4393 (2011).
14. J. Zhong, H. Chen, G. Saraf, Y. Lu, C. K. Choi, J. J. Song, D. Mackie, and H. Shen, "Integrated ZnO nanotips on GaN light emitting diodes for enhanced emission efficiency," *Appl. Phys. Lett.* **90**(20), 203515 (2007).
15. Y. C. Chao, C. Y. Chen, C. A. Lin, Y. A. Dai, and J. H. He, "Antireflection effect of ZnO nanorods arrays," *J. Mater. Chem.* **20**(37), 8134–8138 (2010).
16. D. H. Raguin and G. M. Morris, "Antireflection structured surfaces for the infrared spectral region," *Appl. Opt.* **32**(7), 1154–1167 (1993).
17. B. Thornton, "Limit of the moth's eye principle and other impedance-matching corrugations for solar-absorber design," *J. Opt. Soc. Am.* **65**(3), 267–270 (1975).
18. H. Wahab, A. Salama, A. El-Saeid, O. Nur, M. Willander, and I. Battisha, "Optical, structural and morphological studies of (ZnO) nano-rod thin films for biosensor applications using sol gel technique," *Result Phys.* **3**, 46–51 (2013).

1. Introduction

Thin film solar cells are one of the attractive technologies for generating electrical energy by absorbing photons from sunlight. Among all technologies, polycrystalline $\text{Cu}(\text{In,Ga})\text{Se}_2$ (CIGSe) thin films are considered to be a highly promising candidate for its high absorption coefficient, stability, and suitable band gap [1–3]. To realize a mass-producible energy application, the selenization process is a cost-effective and large-scale method to fabricate CIGSe thin films [4,5]. Aluminum-doped ZnO (AZO) is a promising transparent conductive oxide (TCO) material for the window layer of CIGSe devices due to its environmental friendly and low cost [6]. However, before being excited in the absorber, photons experience an optical loss due to the refractive index difference at the interface between air (refractive index, $n = 1$) and the AZO window layer ($n > 1$) of the device. This optical loss, induced by surface reflection, is one of the loss factors in energy conversion [7,8]. Efficiency-boosting techniques such as antireflection coatings to increase incident photons are highly desired. The MgF_2 thin film is a typical antireflection coating to suppress interference and surface light reflection in a certain wavelength range, but requires time-consuming and high-vacuum deposition [9]. Nevertheless, the subwavelength structure is another approach to enhance light trapping via gradient refractive index profiles between air and the window layer (AZO, in this case). ZnO nanostructure as an antireflection coating is attractive for CIGSe solar cells due to its appropriate refractive index ($n = 2$) and substantially transparent for photons with energy lower than ZnO band edge of 3.2 eV at room temperature [10].

The hydrothermal bottom-up growth is a non-vacuum and low cost technique to prepare ZnO nanorods (NR) [8,11,12]. Recently, several research groups have demonstrated the antireflection coating performance of ZnO NR for improving solar cell efficiency [8,11]. However, the growth time of ZnO NR to efficiently enhance the cell efficiency is currently ranged from 60 to 180 minutes, and more effective fabrication methods must be considered. In addition, it should be noticed that the incident photons would be partially absorbed with the increase of thickness of ZnO NR. The optical transmittance, representing the photon excitation in the absorber, shall be investigated for contributing the photovoltaic performances.

In this study, we demonstrated an efficiency enhancement of CIGSe solar cells by employing ZnO NR structures, fabricated by an efficient non-vacuum solution process in 8 minutes. The optical, morphological, and electrical properties of the CIGSe devices with ZnO NR structures were characterized. The absorption effect of ZnO NR on the photovoltaic efficiency was investigated.

2. Experimental details

The CIGSe thin film solar cells, introduced to the ZnO NR investigation, contained AZO/i-ZnO/CdS/CIGSe/Mo multilayers on a soda-lime glass (SLG) substrate, as shown in Fig. 1(a). A bi-layered Mo electrode of 0.9- μm -thick was deposited by a DC magnetron sputtering system. CIGSe thin films were prepared from the selenization of sputtered metallic

precursors. To enhance the crystallization of chalcopyrite CIGSe thin films, bi-layered metallic precursors were employed using two CuInGa alloy targets for the sputtering system. A conventional precursor layer of the compositional ratio of Ga/(In + Ga) \sim 0.28 was deposited on the Mo-coated SLG substrate, and subsequently covered by an ultra-thin precursor layer of Ga/(In + Ga) \sim 0.60. The selenization was performed in an evaporation system to supply selenium vapors for the precursor-coated substrates, and the substrates were heated to over 540°C at a ramping rate of 20°C/min to form CIGSe thin films. An additional etching step was performed in a KCN-containing aqueous solution (10% KCN) to remove segregated Cu_xSe on the surface. The elemental composition ratio of the CIGSe thin film was confirmed at the ratios of Cu/(In + Ga) \sim 0.90 and Ga/(In + Ga) \sim 0.32, and the thickness was about 1.9 μ m. The 60-nm-thick CdS layer was grown by chemical bath deposition (CBD) at 65°C, and the i-ZnO layer with a thickness of 80 nm was deposited by a radio frequency (RF) magnetron sputtering. To enhance optical and electrical properties of AZO thin film, the deposition was performed by a DC magnetron sputtering system with a substrate heater. The AZO window layer of 420-nm-thick was deposited at the substrate temperature of 80°C.

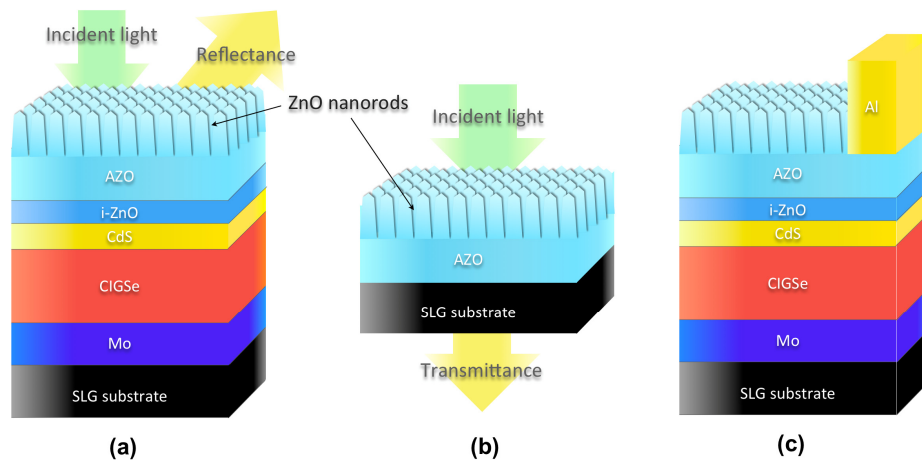


Fig. 1. Schematic of reflectance and transmittance analyses for (a) CIGSe solar cells and (b) AZO-coated SLG substrates covered with ZnO nanorods, respectively. (c) The structure of CIGSe device with Al contact and ZnO NR used for J-V characteristics.

The growth of ZnO NR was to prepare a subwavelength structure on the top of the CIGSe devices, and AZO window layer served as a seed layer for the hydrothermal growth of ZnO NR (AZO/NR). CIGSe devices were immersed in the aqueous solution of zinc nitrate hexahydrate ($\text{Zn}(\text{NO}_3)_2 \cdot 6\text{H}_2\text{O}$) and hexamethylenetetramine ($\text{C}_6\text{H}_{12}\text{N}_4$, HMT) mixture of the concentration of 0.04 and 0.01 M, respectively. The solution was heated to 95°C for the preparation of ZnO NR, and the growth time was ranged from 8 to 25 minutes to evaluate its effect on CIGSe solar cell performances. After completing the NR growth, all devices were cleaned with deionized water to remove residual salt. On the other hand, to investigate the absorption effect, bare AZO-coated SLG substrates were also immersed in the solution for 8 to 25 minutes to prepare the same ZnO NR for optical analyses, as shown in Fig. 1(b). For J-V measurement, individual cells with the area of 0.4 cm^2 were defined by mechanical scribing. To efficiently collect photocurrent of CIGSe devices, Al front contact grid structures (1 μ m in thickness) were evaporated on the top of conductive AZO layer before the growth of ZnO NR, as shown in Fig. 1(c).

The transmittance and reflectance for AZO/NR thin films and the CIGSe devices covered with ZnO NR were respectively measured by UV/VIS spectrophotometer, as shown in Fig. 1. Morphologies were observed by field emission scanning electron microscopy (FESEM, JSM-6500F, JEOL), and the crystallization was analyzed by high resolution X-ray diffractometer (XRD, Bede D1). Effective refractive index was carried out by a spectroscopic ellipsometer

(M-2000, J. A. Woollam Co.). J-V characteristics of the CIGSe solar cells were measured using a solar simulator at one sun illumination of 100 mW/cm^2 with AM 1.5G spectrum (Oriel class A, 91160A, Newport Co.).

3. Results and discussion

3.1 Morphologies and crystalline features

SEM micrographs revealed the morphologies of the CIGSe devices with ZnO NR structures with respect to various growth times, shown in Fig. 2. The as-fabricated device showed dense and smooth surface morphology of bare AZO layer; the surface, however, exhibited anisotropic column-like structures on the top of devices after hydrothermal growth. It was observed that the diameter of the NR structure ranged from 70 to 120 nm in all samples, and the height enlarged with the increase of immersion time of the hydrothermal process. The end of the NR structure was clearly confirmed as a cone-like shape, which could effectively reduce surface reflectance and improve the cell efficiency [8]. The height of NR structures, observed from cross-sectional SEM images, was estimated to 100, 210, 290, and 540 nm for the samples after hydrothermal growth for 8, 11, 14, and 25 minutes, respectively.

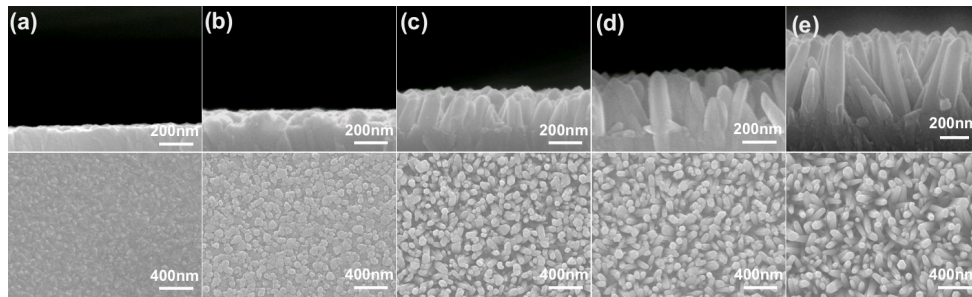


Fig. 2. SEM micrographs of (a) as-fabricated CIGSe devices and after the growth of ZnO nanorods for (b) 8, (c) 11, (d) 14, and (e) 25 minutes.

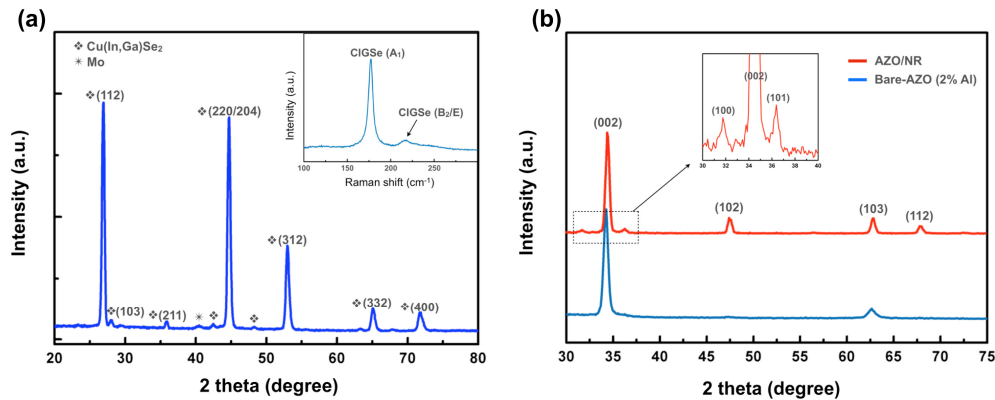


Fig. 3. X-ray diffraction patterns of (a) CIGSe absorber, and (b) bare AZO thin film covered with ZnO nanorods. Inset in Fig. 3(a) shows Raman scans of CIGSe absorber.

To identify the crystalline characteristics of CIGSe devices and NR coatings, the CIGSe absorber, bare AZO, and AZO/NR thin films were measured by X-ray diffraction. XRD pattern of 1.9- μm -thick absorber revealed the growth of chalcopyrite CIGSe phase with strong (112) and (220/204) preferred orientation, as shown in Fig. 3(a). The dominant peaks of (112) at 26.9° and (220/204) at 44.6° represented the elemental composition ratio of $\text{Ga}/(\text{In} + \text{Ga}) \sim 0.3$. Moreover, the Raman scans, shown in the inset of Fig. 3(a), revealed no segregated Cu_xSe phase on the surface of CIGSe absorbers due to the absence of the peak at 260 cm^{-1}

[13]. Figure 3(b) shows the XRD patterns for bare AZO and AZO/NR thin films. The blue curve revealed aluminum-doped ZnO phase with a strong peak at 34.5° in the bare AZO thin film. In comparison to intrinsic ZnO phase, a small shift in a diffraction angle was observed, attributed to the substitution of Al^{3+} ions for Zn^{2+} ions in the ZnO lattice during deposition [11]. In addition, AZO/NR thin film exhibited the peaks at 31.7° , 36.2° , 47.5° , and 67.9° (see red curve), representing (100), (101), (102), and (112) oriented wurtzite ZnO phase, respectively, confirmed the growth of ZnO NR.

3.2 Optical analyses for ZnO nanorods structures

The gradient refractive index profiles, contributed by the subwavelength structure, have been numerically simulated [7,14]. Nevertheless, the refractive index varied through the ZnO NR can be further explored. To further identify the effective refraction index profiles experimentally, the AZO/NR thin film was examined by spectroscopic ellipsometer. It should be mentioned that the diffusive reflection was considered for the sample covered with ZnO NR; nevertheless, a dominant specular reflection was still expected to ensure the accuracy of ellipsometer measurement [15]. After automatic fitting, the analytic results for ZnO NR were divided into two effective areas: Top-NR and Bottom-NR. The wavelength-dependent in-depth variation of refractive index was plotted in Fig. 4. The refractive index of bulk AZO thin film varied from 2.01 to 1.65 in the wavelength range between 400 and 1000 nm. For the ZnO NR, refractive index profiles varied from 1.70 to 1.53 for the Bottom-NR area, and from 1.51 to 1.41 for the Top-NR. The in-depth gradient of refractive index was achieved by covering the ZnO NR structure on the top of AZO seed layer.

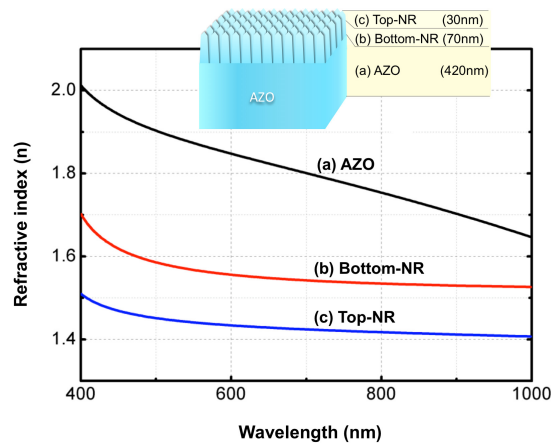


Fig. 4. Wavelength-dependent refractive index profiles of (a) AZO, (b) Bottom-NR, and (c) Top-NR areas for the AZO film covered with ZnO nanorods.

The effect of ZnO NR on the antireflection coating performance was carried out by optical reflectance and transmittance analyses. An optimized NR structure to effectively reduce surface reflectance of incident light must fulfill following conditions [7,8,16,17]:

- (1) The height (h) must not be smaller than 40% of the longest operational wavelength (λ): $h \geq 0.4\lambda$.
- (2) The center-to-center spacing (Λ) of the NR structure must be smaller than the shortest operational wavelength (λ) divided by material refractive index (n): $\Lambda < \lambda/n$.

It was concluded that the height of ZnO NR structure be higher than 400 nm to effectively reduce the surface reflectance at the operational wavelengths from 400 to 1000 nm. Therefore, except for the bare CIGSe device, the interference fringes and relatively high light reflectance were noticeably observed in the samples with 100 and 210-nm-height ZnO NR due to inadequate heights, as shown in Fig. 5(a). Moreover, the obvious reduction of surface light

reflectance was observed in the shorter operational wavelength range in comparison with that in the range of longer one, which can be explained by the factor from antireflection coating according to the ratio of NR height to operational wavelength. The bare CIGSe device exhibited obvious surface light reflection, and the average reflectance was calculated to be 14.5% in the wavelength range between 400 and 1000 nm. On the other hand, the average reflectance was reduced to 7.0%, 4.6%, 3.4%, and 2.3% after employing ZnO NR for the height of about 100, 210, 290, and 540 nm, respectively. It was expected that the lower the surface reflection of incident light, the higher the efficiency of CIGSe solar cells was achieved. However, ZnO dielectric material exhibits partially absorption over the visible spectrum (400 to 700 nm) with the increase of thickness, and the absorbance from ZnO NR is shown in the inset of Fig. 5(b) [18]. ZnO semiconductor material with direct band gap of 3.2 eV possesses high UV absorption at wavelengths lower than 400 nm, and reveals a step decrease of absorbance around the absorption edge. This absorption effect, thus, is considered to reduce the transmittance of incident photons in the visible light spectrum.

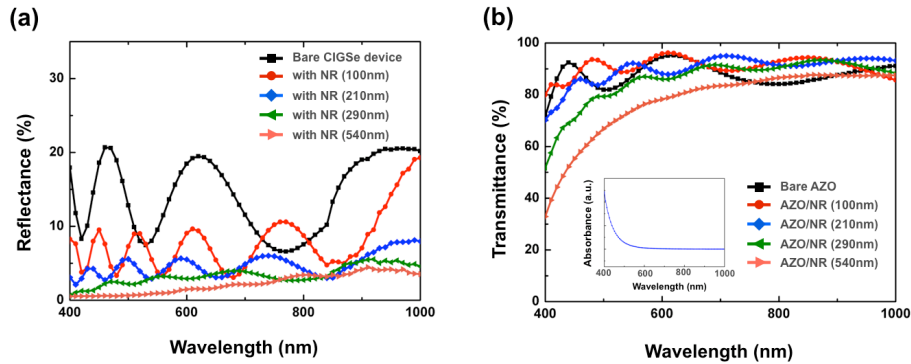


Fig. 5. (a) Surface reflectance of the as-fabricated CIGSe solar cell and covered with ZnO nanorods, and (b) transmittance analyses of AZO/NR thin films. The absorbance of ZnO nanorods is shown in the inset of Fig. 5(b).

To investigate the absorption effect of the ZnO NR, the optical transmittance of the bare AZO and AZO/NR thin films was examined and illustrated in Fig. 5(b). The average transmittance of bare AZO thin film was calculated to be 89.2% at the wavelengths from 400 to 1000 nm, and improved to 92.4% after covered with 100-nm-height ZnO NR. This improvement, contributed by employing the NR structure on the top of AZO thin film, was concluded to increase the photocurrent of the CIGSe device. However, the transmittance of the AZO/NR thin films of 210, 290, 540 nm in NR height decreased to 91.5%, 87.2% and 79.0%, respectively. Even the surface light reflectance could be further reduced via the increase of height of ZnO NR, as shown in Fig. 5(a); the transmittance was hardly improved accordingly, and reduced to as low as 79.0% for the sample with 540-nm-height ZnO NR. From the transmittance decrease in the range of visible light spectrum, the evidence of absorption effect from ZnO NR was observed [see the inset in Fig. 5(b)]. In summary, the 540-nm-height ZnO NR exhibited the best antireflection function for the lowest surface reflectance among all samples; the 100-nm-height ZnO NR, however, provided the highest transmittance of incident photons to enhance solar cell efficiency.

3.3 J-V characteristics for CIGSe solar cells

J-V characteristic was examined to evaluate the effect of ZnO NR antireflection coating on CIGSe devices, as plotted in Fig. 6. The results indicated that no significant difference of open circuit voltage (V_{OC}) but a variation of short-circuit current density (J_{SC}) was observed, contributed by the increase of incident photons. Table 1 lists the electrical parameters for all CIGS devices with and without ZnO NR coating. Five as-fabricated CIGSe solar cells prepared from the same batch presented the conversion efficiency and J_{SC} of approximate

9.4% and 31.7 mA/cm², respectively. After covered with 100-nm-height ZnO NR on the top of devices, efficiency and J_{SC} were improved to 10.1% and 34.5 mA/cm², respectively. This photocurrent increase, related to the increase of photon excitation in the CIGSe absorber, enhanced photovoltaic efficiency after introducing ZnO NR antireflection coatings. However, the performances of CIGSe solar cells were not further enhanced according to further reflectance reduction in other samples. The efficiency and J_{SC} respectively decreased to 8.8% and 29.5 mA/cm² in the device covered with ZnO NR of 540 nm in height, attributed to the optical absorption from ZnO NR.

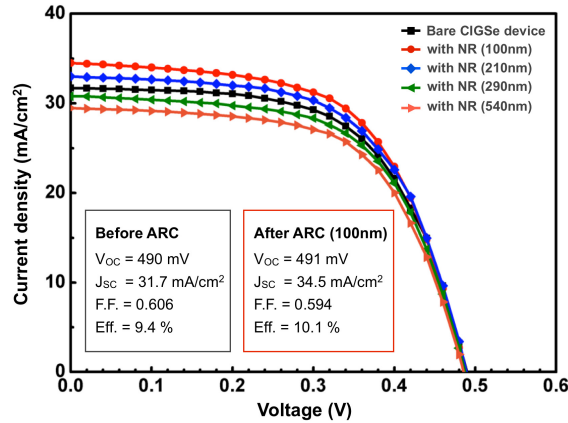


Fig. 6. J–V characteristics of the bare CIGSe device and the devices with ZnO nanorods.

Table 1. The photovoltaic performances of the CIGSe solar cells with different conditions of ZnO nanorods antireflection coatings

Device ID	ZnO NR structure		Electrical properties				
	Growth time (min)	Height (nm)	V _{OC} (mV)	Fill Factor (%)	J _{SC} (mA/cm ²)	η (%)	Improvement (η) (%)
1	-	-	490	60.6	31.7	9.4	-
2	8	100	491	59.4	34.5	10.1	+ 7.4
3	11	210	490	60.1	33.0	9.7	+ 3.2
4	14	290	491	61.2	30.8	9.3	- 1.1
5	25	540	490	60.6	29.5	8.8	- 6.4

5. Conclusion

A ZnO NR subwavelength structure, prepared by an efficient non-vacuum solution process in 8 minutes, yielded the in-depth gradient of refractive index profile to increase incident photons and photocurrent of CIGSe solar cells. The surface reflectance of CIGSe devices could be effectively reduced via increasing the height of ZnO NR. However, the transmittance of incident light decreased according to the increase of NR height due to its absorption loss, resulting in low J_{SC} and conversion efficiency. The highest efficiency enhancement of CIGSe solar cells by 7.4% referred to J_{SC} increase by 8.8% was achieved by introducing 100-nm-height ZnO NR structure, even if its antireflection function was not the highest among all samples. However, the decrease of J_{SC} by 6.9% was observed to decrease solar cell efficiency by 6.4% in the device with 540-nm-height ZnO NR. The advantages of ZnO NR antireflection coating for improving photovoltaic efficiency of CIGSe solar cells are significant. This antireflection technology is expected to benefit light collecting for improving energy conversion in not only CIGSe solar cells but also other photovoltaic devices with ZnO-based

window layers. Moreover, by optimizing growth conditions and the geometry of the ZnO NR with low absorption effect, further improvement of photovoltaic performances can be expected.

Acknowledgment

The authors would like to thank National Nano Device Laboratories (NDL), Taiwan for technical supports of optical analyses.